JACS
JOURNAL OF THE AMERICAN CHEMICAL SOCIETY

Article

pubs.acs.org/JACS

Ordered Phosphorylation Events in Two Independent Cascades of the PTEN C-tail Revealed by NMR

Florence Cordier,*[,†,‡] Alain Chaffotte,[†,‡] Elouan Terrien,[†,‡,§] Christophe Préhaud,[⊥,∥] François-Xavier Theillet,[†,‡,□] Muriel Delepierre,[†,‡] Monique Lafon,[⊥,∥] Henri Buc,[¶] and Nicolas Wolff[†,‡]

Département de Biologie Structurale et Chimie, [†]Unité de Résonance Magnétique Nucléaire des Biomolécules, Institut Pasteur, F-75015 Paris, France

[‡]CNRS, UMR3528, F-75015 Paris, France

[§]Cellule Pasteur UPMC, University of Pierre and Marie Curie, rue du Dr Roux, 75015 Paris, France

Département de Virologie, [⊥]Unité de Neuroimmunologie Virale, Institut Pasteur, F-75015 Paris, France

[∥]CNRS, URA3015, F-75015 Paris, France

[¶]Institut Pasteur, F-75015 Paris, France

Supporting Information

ABSTRACT: PTEN phosphatase is a tumor suppressor controlling notably cell growth, proliferation and survival. The multisite phosphorylation of the PTEN C-terminal tail regulates PTEN activity and intracellular trafficking. The dynamical nature of such regulatory events represents a crucial dimension for timing cellular decisions. Here we show that NMR spectroscopy allows reporting on the order and kinetics of clustered multisite phosphorylation events. We first unambiguously identify *in vitro* seven *bona fide* sites modified by CK2 and GSK3β kinases and two new sites on the PTEN C-terminal tail. Then, monitoring the formation of transient intermediate phosphorylated states, we determine the sequence of these reactions and calculate their apparent rate constants. Finally, we assess the dynamic formation of these phosphorylation events induced by endogenous kinases directly in extracts of human neuroblastoma cells. Taken together, our data indicate that two cascades of events controlled by CK2 and GSK3β occur independently on two clusters of sites (S380−S385 and S361−S370) and that in each cluster the reactions follow an ordered model with a distributive kinetic mechanism. Besides emphasizing the ability of NMR to quantitatively and dynamically follow post-translational modifications, these results bring a temporal dimension on the establishment of PTEN phosphorylation cascades.

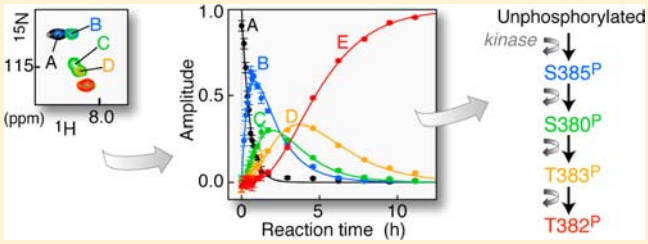

INTRODUCTION

The dual lipid and protein phosphatase PTEN is a tumor suppressor playing a pivotal role notably in controlling cell growth, proliferation and neuro-survival.[1,2] PTEN consists of four major domains, a PIP2-binding module participating in membrane association, a phosphatase domain required for its enzymatic activity, a C2 domain involved in membrane phosphatidylserine binding and a long flexible and unfolded C-terminal tail (PTEN-Ctail, residues 351−403, see sequence in Figure 5). The phosphorylation at several Ser/Thr residues of PTEN-Ctail constitutes an essential regulatory mechanism controlling PTEN activity, stability, cellular localization and interaction with scaffold proteins. PTEN-Ctail phosphorylation has been extensively studied *in vitro* and in various cell lines, using classical techniques (see refs 3 and 4 for review). However, these techniques bear weaknesses, e.g., in discerning phosphorylation events occurring in close vicinity in the sequence. Therefore, depending on the technique used and experimental conditions, different subsets of sites are detected, making comparative analyses and functional interpretations difficult. Taken together, these studies reveal seven sites, which are modified to various extents, S370, S380, T382, T383 and S385 by casein kinase 2 (CK2)[5−11] and S362, T366 by glycogen synthase kinase-3 β (GSK3β).[9,12] Polo-like kinase 3 (Plk3) was recently reported to phosphorylate PTEN both at T366 and S370.[13] Other Ser/Thr kinases, such as the microtubule-associated serine/threonine (MAST) family,[14] serine/threonine kinase 11 (STK11 also named LKB1)[15] and casein kinase 1 (CK1)[12] have been shown to be implicated, but on unidentified sites. Several mutant-based studies reported that phosphorylation within the entire S380−S385 cluster is crucial to stabilize PTEN, to prevent its interaction with binding partners and to reduce its membrane localization and catalytic activity.[5−8,10,11] However, the function of T366 and S370 is less clear. Phosphorylation on T366 by GSK3β led to destabilization of PTEN[16] and may provide negative feedback regulation of PTEN.[12] Controversially, phosphorylation of

Received: October 16, 2012
Published: November 21, 2012

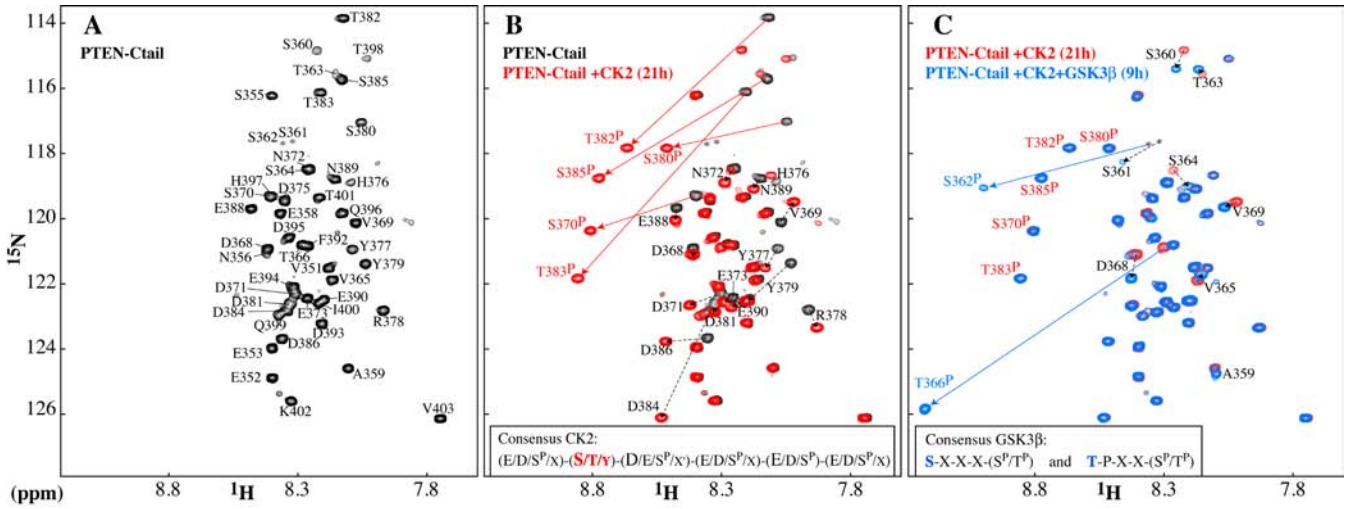

Figure 1. Unambiguous identification of PTEN-Ctail phosphorylation sites *in vitro* by NMR chemical shift perturbations. (A) Assigned $^{1}H-^{15}N$ HSQC spectrum of $^{15}N/^{13}C$-labeled unphosphorylated PTEN-Ctail (black, 120 μM, pH 6.7, 25 °C). Amide resonances appearing below the threshold level of the plot are indicated by a star (*). (B) In red, spectrum recorded 21 h after addition of CK2 kinase to the PTEN-Ctail sample (black). Resonances of phosphorylated Ser/Thr residues by CK2 are labeled in red, and slightly shifted neighboring resonances, in black. (Inset) Consensus phosphorylation sequence of CK2, where X is any residue except basic residues and X′ is any residue except basic or proline residues; the size of the letters is roughly proportional to the frequency of a given residue at that position.[17] (C) In blue, spectrum recorded 9 h after addition of GSK3β kinase to the CK2-phosphorylated PTEN-Ctail sample (red). Resonances of phosphorylated Ser/Thr residues by GSK3β are labeled in blue, and slightly shifted neighboring resonances, in black. (Inset) Consensus phosphorylation sequence of GSK3β.[18,19]

S370 and T366 by Plk3 was shown recently to stabilize PTEN and increase its activity.[13]

Multiphosphorylation events provide a reversible molecular mechanism to time cellular events. Crucial cellular decisions such as the trigger of cellular survival are probably governed by such finely tuned regulatory events. The system involving kinases, phosphatases and substrate is likely maintained far from equilibrium *in vivo*, so that tiny changes in their local concentration lead to drastic changes in cell fate. To better understand the biological relevance of PTEN modifications in a particular cell type and to bring a temporal dimension to these events, a complete and dynamical description in terms of phosphorylation order and kinetics is needed. Recent mass spectrometry-based techniques, such as AQUA or FLEXIQuant strategies using fragmentation methods, allow identifying and quantifying the phosphorylation state of peptides and proteins at the residue level.[20−22] However, such a residue-specific approach is somewhat difficult to set up, in particular when numerous and/or clustered sites are concerned and/or when working with cell extracts. Alternatively, phosphorylation events can be detected by high-resolution NMR spectroscopy *in vitro*, in cellular extracts and even in intact oocytes cells.[23] Indeed, NMR has recently demonstrated its suitability to monitor post-translational events in a time-dependent manner on entire peptides or proteins[23−26] and to report on stepwise modifications at the residue level.

In this contribution, we show that NMR further allows reporting on the dynamic nature of clustered multisite phosphorylation events *in vitro* and in extracts of human neuroblastoma cells. By following the formation of transient intermediate phosphorylated states in the NMR spectra, we show that two cascades of phosphorylation events occur independently and that, in each cascade, the reaction proceeds in a defined order *via* a distributive mechanism. These results shed new light on the dynamical process of PTEN multisite phosphorylation.

RESULTS

Unambiguous Identification of Seven *Bona Fide* CK2 and GSK3β Phosphorylation Sites on PTEN-Ctail *in Vitro* by NMR. To identify PTEN-Ctail phosphorylation sites by NMR, recombinant U−$^{15}N/^{13}C$-labeled PTEN-Ctail (residues V351−V403 of human PTEN, see sequence in Figure 5) was produced in *Escherichia coli*. The NMR $^{1}H-^{15}N$ heteronuclear single quantum correlation (HSQC) spectrum recorded on PTEN-Ctail showed very limited dispersion of amide resonances (Figure 1A), characteristic of an unfolded peptide. To monitor by NMR the phosphorylation of PTEN-Ctail by CK2 kinase *in vitro*, experimental conditions leading to a detectable amount of phosphorylation were initially set up by mass spectrometry. Thus, an adjusted amount of recombinant CK2 was added to the PTEN-Ctail NMR sample as described in Materials and Methods. $^{1}H-^{15}N$ HSQC spectra were regularly recorded in the time course of the reaction and showed the appearance of new resonance signals and the disappearance of others (Figure 1B), in agreement with the high sensitivity of ^{1}H and ^{15}N chemical shifts toward phosphorylation-induced changes in the neighborhood of a phosphorylated residue. After 21 h of reaction, when no more spectral changes were visible, resonance assignment of the phosphorylated form of PTEN-Ctail using a set of 3D NMR experiments allowed unambiguous identification of the most strongly downfield shifted resonances as a first set of CK2-phosphorylated residues $S370^{P}$, $S380^{P}$, $T382^{P}$, $T383^{P}$ and $S385^{P}$ (see sequence in Figure 5). Each of these five sites lies within a CK2 consensus motif,[17] where an acidic or phosphorylated residue is invariably found at position either $n + 1$ or $n + 3$ of the CK2 site (Figure 1B, Inset). Other slightly shifted resonances were assigned to neighbors of these phosphorylated Ser/Thr residues (see also Figure S1, in Supporting Information [SI]).

Phosphorylation of PTEN-Ctail by GSK3β kinase was similarly assessed by mass spectrometry. No phosphorylation

dx.doi.org/10.1021/ja310214g | J. Am. Chem. Soc. 2012, 134, 20533−20543

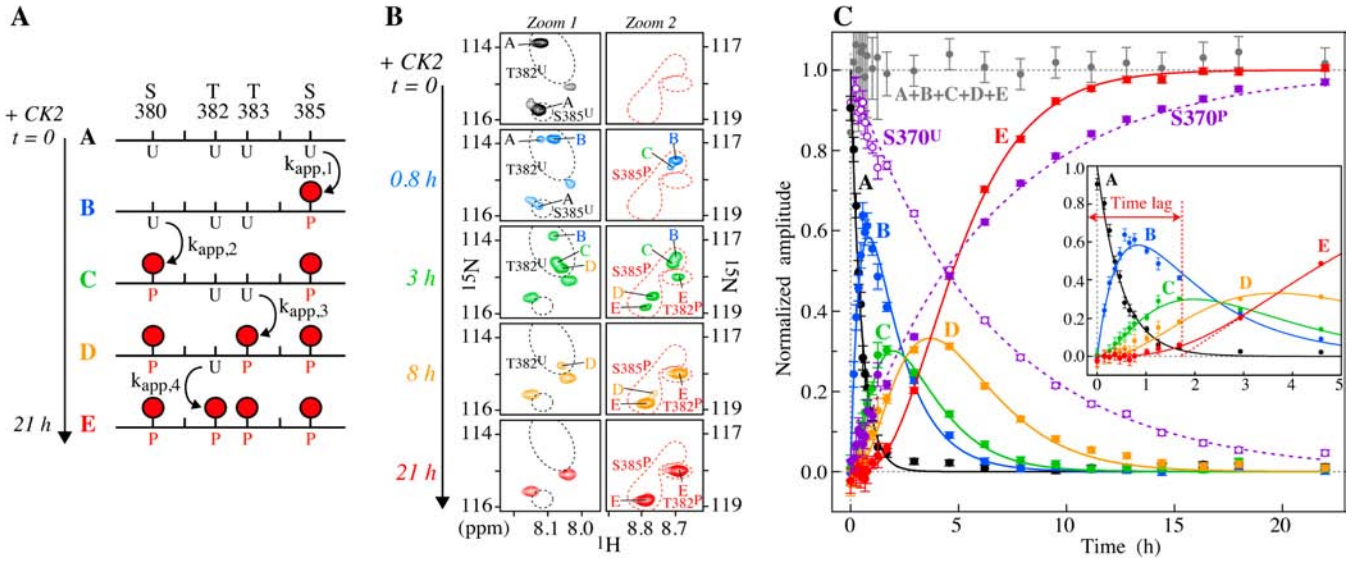

Figure 2. Kinetics of the multisite phosphorylation events in the S380−S385 cluster of PTEN-Ctail by CK2 *in vitro*. (A) Definition of the phosphoforms within the S380−S385 cluster as they appear in time in the sequential reaction model (from species A to E). U or P denotes unphosphorylated or phosphorylated by CK2. (B) Two representative regions of the unphosphorylated and phosphorylated regions (zoom 1 and zoom 2, respectively) of the $^{1}H-^{15}N$ HSQC spectra of $^{15}N/^{13}C$-labeled PTEN-Ctail recorded in the time course of the CK2 reaction from 0 to 21 h (from top to bottom). Resonance assignment is indicated for the resonances of $T382^{U}$ in species A−D and $S385^{U}$ in species A in zoom 1 and for the resonances of $T382^{P}$ in species E and $S385^{P}$ in species B, C, D and E. (C) Amplitudes of the averaged normalized resonance signals for each species A to E (and their sum) are plotted as a function of the CK2 reaction time. Error bars correspond to the rms of the noise in the corresponding spectrum. The curves (solid lines) are the result of a global nonlinear least-squares fitting of the amplitudes *A*−*E* to eqs (1a)−(1e) given in SI. The time lags introduced by such an ordered process can be appreciated in the Inset, which represents a zoom on the first 5 h. The time course of the normalized amplitude of $S370^{U}$ and $S370^{P}$ resonances (open and filled violet circles) was fitted to single exponential functions (dashed lines).

could be detected by GSK3β unless CK2 was simultaneously added in the sample. This observation corroborates the fact that GSK3β usually requires an initial priming phosphorylation, optimally located four residues downstream, by another kinase (Figure 1C, Inset).[18,19] Thus, phosphorylation of PTEN-Ctail by GSK3β was monitored by NMR by adding an adjusted amount of recombinant GSK3β to the CK2-phosphorylated PTEN-Ctail sample (see Materials and Methods). Again, a series of $^{1}H-^{15}N$ HSQC spectra was acquired in the time course of the reaction. After 9 h, two resonances were drastically downfield shifted and were unambiguously assigned to the phosphorylated residues $S362^{P}$ and $T366^{P}$ (Figure 1C). As anticipated from the GSK3β consensus site, these results suggest that priming phosphorylation by CK2 at S370 allows GSK3β to first modify T366 (as originally proposed by Maccario et *al.*[16]) and then S362 (see sequence in Figure 5). The few slightly shifted resonances correspond to neighboring residues A359-V369. By simultaneously adding CK2 and GSK3β, the same NMR spectra were obtained at the end of the reaction (see Figure S1 in SI).

Thus, our data allow unambiguous identification of seven *bona fide* phosphorylation sites in PTEN-Ctail *in vitro*, modified by CK2 at S370, S380, T382, T383 and S385 and by GSK3β at S362 and T366.

Evidence of a Distributive Ordered Phosphorylation Mechanism in the S380−S385 Cluster of PTEN-Ctail and Apparent Rate Constants of the Reactions. In the series of HSQC spectra acquired during the CK2 reaction (see two representative regions in Figure 2B and an overlay of the full spectra in Figure S2 [SI]), we observed the progressive disappearance of the resonances of the unphosphorylated PTEN-Ctail species (denoted A) and the appearance of the resonances of the fully phosphorylated species within the S380−S385 cluster (denoted E) and, meanwhile, the appearance and subsequent disappearance of resonances of three intermediate phosphorylated species (denoted B, C and D). The species A−E correspond to unphosphorylated (A), mono-$S385^{P}$ (B), bi-$S385^{P}$-$S380^{P}$ (C), tri-$S385^{P}$-$S380^{P}$-$T383^{P}$ (D) and fully phosphorylated $S385^{P}$-$S380^{P}$-$T383^{P}$-$T382^{P}$ species (E), as described in Figure 2A. Our data indicate that the phosphorylation events within this cluster proceed in a precise order, at sites S385, S380, T383 and T382, *via* the transient accumulation of three unique intermediate phosphorylated states according to the following sequential reaction model:

$$A \xrightarrow{k_{app,1}^{S385}} B \xrightarrow{k_{app,2}^{S380}} C \xrightarrow{k_{app,3}^{T383}} D \xrightarrow{k_{app,4}^{T382}} E \quad (1)$$

We unambiguously came to this conclusion for the following four reasons: In the series of HSQC spectra, we observed that, (i) upon phosphorylation of S385 (species A to B), the decay in amplitude of $S385^{U}$(A) (the unphosphorylated S385 resonance peak in species A) was concomitant with a transient increase in amplitude of phosphorylated $S385^{P}$ (B). Due to the influence of phosphorylation of a residue on its neighbors (up to $n \pm 5$), the phosphorylation of S385 led to the slight synchronous resonance shift of unphosphorylated $S380^{U}$, $T382^{U}$ and $T383^{U}$, which disappeared from species A to concomitantly reappear as species B. Then, (ii) phosphorylation of S380 gave rise to a transient accumulation of phosphorylated $S380^{P}$ (C) and a concomitant disappearance of $S380^{U}$ (B), accompanied by a small shift of the neighboring $T382^{U}$, $T383^{U}$ and $S385^{P}$ resonances, which disappeared from species B to reappear as species C. According to a similar "transient/concomitant" process, (iii) phosphorylation of T383 led to an accumulation of $T383^{P}$ (D), a disappearance of $T383^{U}$ (C) and a slight shift

dx.doi.org/10.1021/ja310214g | J. Am. Chem. Soc. 2012, 134, 20533−20543

Table 1. Apparent Rate Constants (h^{-1}) of Each Event within the Two Cascades for the *in Vitro* Experiment[a]

cluster 1	**S385**[b] 1.93 ± 0.29	**S380**[b] 0.65 ± 0.01	**T383**[b] 0.82 ± 0.05	**T382**[b] 0.50 ± 0.04	
cluster 2	**S370**[b] 0.15 ± 0.01	***T366***[c] *0.43 ± 0.03*	***S362***[c] *0.19 ± 0.01*	**S361**[b] 0.012 ± 0.001	**T363**[b,d] <0.006 ± 0.001

[a]Values of the apparent rate constants (in h^{-1}) depend on the concentration of kinases and substrate. Details on the fitting procedure are given in Materials and Methods and in the Supporting Information. [b]CK2 phosphorylation events. [c]GSK3β phosphorylation events in italic, occurring on a different time scale than the CK2 ones. [d]Poor accuracy on this apparent rate constant, since the decay of species D′ is not sampled.

of its neighbors $S380^P$, $T382^U$ and $S385^P$, which disappeared from species C to reappear as species D. Finally, (iv) phosphorylation of T382 led to an increase in intensity of $T382^P$ (E) up to a stable plateau, a disappearance of $T382^U$ (D) and a slight shift of $S380^P$, $T383^P$ and $S385^P$, which disappeared from species D to reappear, also up to a plateau, as species E. This succession of time-coupled events demonstrates that the phosphorylation of the S380−S385 cluster obeys the following ordered process: $\rightarrow S385^P \rightarrow S380^P \rightarrow T383^P \rightarrow T382^P$. Neither other branched phosphorylation models nor random mechanisms could explain our data: In summary, as schematized in Figure 2A, a unique resonance signal is observed in the overlay of HSQC for $S385^U$ (species A), and four resonances are observed for $S385^P$ (B, C, D and E). Similarly, two signals are observed for $S380^U$ (A, B), and three signals are observed for $S380^P$ (C, D, E). Three signals are observed for $T383^U$ (A, B, C), and two signals are observed for $T383^P$ (D, E). Finally, four signals are observed for $T382^U$ (A, B, C, D), and a single signal is observed for $T382^P$ (E). Thus, the kinetic decay of A can be deduced not only from the resonance amplitude of $S385^U$ but also from that of neighboring residues whose chemical shifts are influenced by the phosphorylation at the 385 position. The same situation applies for B to E species. Assignment of these intermediate resonances could be unambiguously established on the basis of the fact that (i) chemical shift changes of a residue from a species to the next one are generally decreasing with increasing distance to the phosphorylated site (see Figure S1 in SI) and (ii) the time course of disappearance/appearance of each species as "seen" from different residues follows the same kinetics (see below).

The observation of these intermediate species on the NMR spectra indicates that the substrate must be released from the CK2 kinase active site between each phosphorylation step. In addition, the sum of the resonance amplitudes *A*, *B*, *C*, *D* and *E* is statistically constant over the time of reaction (see Figure 2C). Therefore, our data clearly show that the reaction predominantly obeys a distributive ordered mechanism, in which each of the four phosphorylation steps requires a separate binding event between the kinase and the substrate (in contrast to a processive mechanism without substrate release).

In order to appreciate the relative rates of transfer associated to the successive phosphorylation events, we approximate each elementary step of the linear five-state model mentioned above to a spontaneous (irreversible) first order reaction. According to this approximation, the time course of the disappearance/appearance of the resonance amplitudes *A*, *B*, *C*, *D* and *E* of residues in each species is given by a sum of exponential functions (as given by eqs (1a)−(1e) of the SI) that depend on A_0, the initial amplitude of species A (with $A_0 = A + B + C + D + E$), and on $k_{app,1}$, $k_{app,2}$, $k_{app,3}$ and $k_{app,4}$, the apparent rate constants (or transfer rate constants) of the S385, S380, T383 and T382 phosphorylation events, respectively. Each apparent rate constant depends on the rates for reversible enzyme binding and for catalysis at a given concentration of substrate and kinase. The sum of the resonance amplitude $A + B + C + D + E$ (for each residue) being statistically constant in the time course of the reaction, the amplitudes were measured and normalized so that $A + B + C + D + E = 1$ for each residue, using a residue-specific A_0 constant. The variation in time of the average amplitude of each species shows the transient nature of the three intermediate phosphorylation species B, C and D and the time lag in the appearance of the C, D, and E species (Figures 2C and Inset). Individual nonlinear least-squares fitting of amplitudes *A*, *B*, *C*, *D* and *E* to their corresponding equation, using a simplex or Levenberg−Marquardt algorithm, allowed extracting $k_{app,1}$, $k_{app,2}$, $k_{app,3}$ and $k_{app,4}$ values of 1.93 ± 0.29, 0.65 ± 0.01, 0.82 ± 0.05 and 0.50 ± 0.04 h^{-1}, respectively, in our conditions (Table 1). These values are very similar to the ones extracted from a global fit of the average *A*−*E* data (Table S1, SI). A detailed description of the fitting procedure is given in Materials and Methods.

A simpler analysis was required to evaluate the kinetics of phosphorylation of S370. As seen in Figure 2C and Figure S2 (SI), $S370^U$ resonance disappears *via* a single exponential decay ($U = U_0\, e^{-k_{app}t}$), while $S370^P$ resonance synchronously appears *via* an exponential function ($P = U_0(1- e^{-k_{app}t})$), with the same apparent rate constant k_{app} and with $U_0 = U + P$ (*U* and *P* the resonance amplitudes of unphosphorylated and phosphorylated species). Note that no initial lag phase is detectable in the accumulation of $S370^P$, suggesting that phosphorylation of this residue occurs as an event independent of the phosphorylation pattern developing in the S380−S385 cluster. To validate this hypothesis, we have produced the S380A/T382A/T383A/S385A PTEN-Ctail mutant and performed an NMR experiment under identical experimental conditions as for the wild type. In this quadruple mutant, the phosphorylation of S370 (and the downstream GSK3β-phosphorylation reactions, see below) proceeds normally as for the wild type (Figure S6 (SI)). Upon S370 phosphorylation of PTEN-Ctail, the neighboring peaks V369 and N372 disappear and reappear with slightly shifted resonance frequencies and with amplitudes fitting to the same equations with the same apparent rate constant as $S370^U$ and $S370^P$. Thus, the apparent rate constant k_{app}^{S370} was extracted from individual nonlinear least-squares fitting of the normalized amplitudes of the representative species $S370^U$ and $S370^P$ to the single exponential functions given above, respectively, giving an average value of 0.15 ± 0.01 h^{-1} in our conditions (Table 1).

In conclusion, by a thorough analysis of the series of HSQC spectra, we show that the CK2 phosphorylation sites are processed in a defined order in the S380−S385 cluster (S385→S380→T383→T382) by a distributive kinetic mechanism and randomly on S370, i.e., independently of the S380−S385 cluster (Figure 5). Our data further allow deriving the five apparent rate constants of each of these CK2 phosphorylation events (at a given concentration of substrate and kinase).

Modifications of PTEN-Ctail by GSK3β and Identification of Additional Late Phosphorylation Sites. While no detectable phosphorylation takes place after addition of GSK3β alone (see above), the GSK3β reaction was followed on

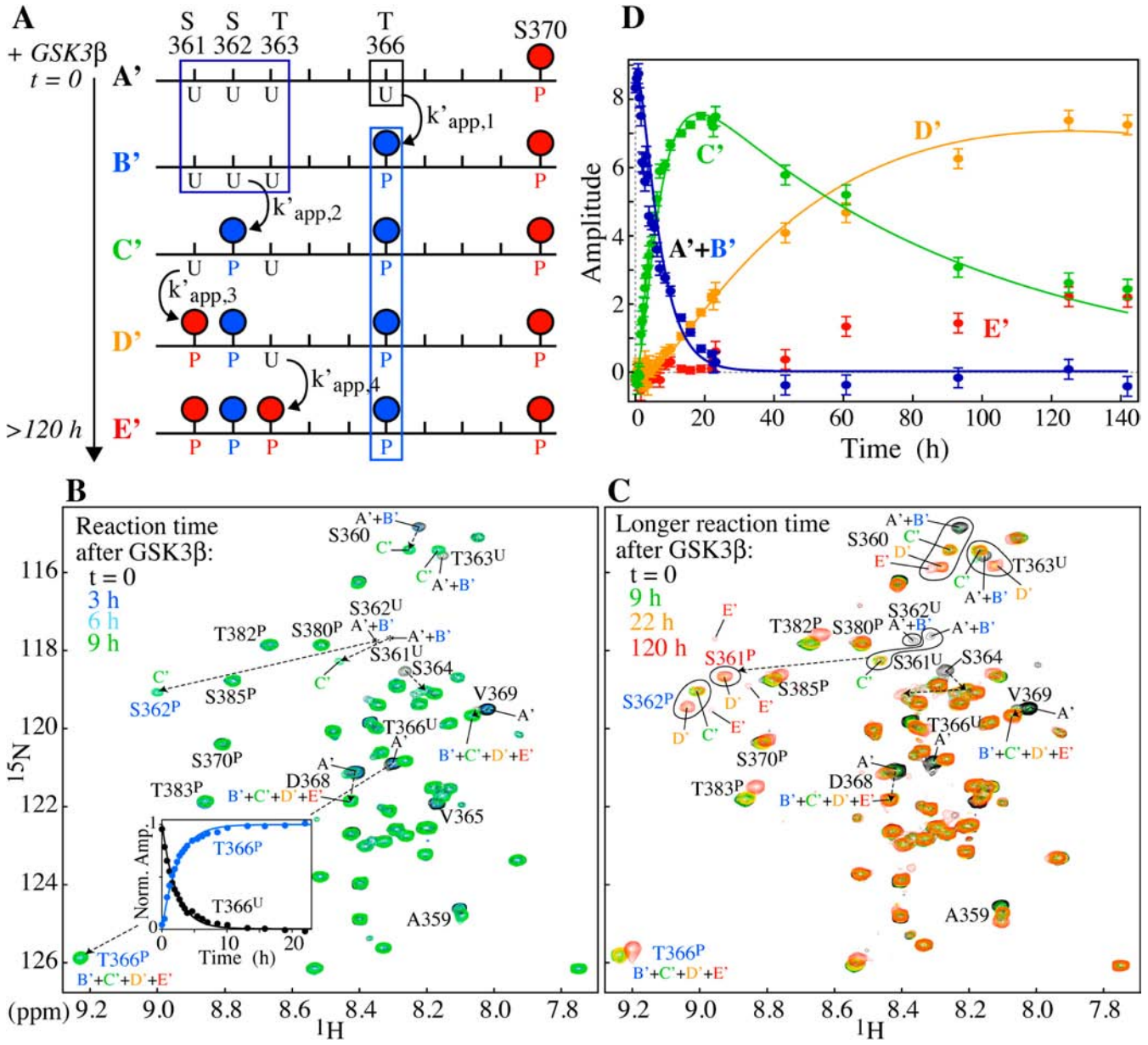

Figure 3. Kinetics of PTEN-Ctail phosphorylation reactions by GSK3β kinase *in vitro* and evidence of late CK2 modifications at two new sites. (A) Definition of the phospho-forms within the S361−T366 cluster as they appear in the sequential reaction model (from species A′−E′). U or P denotes unphosphorylated or phosphorylated state; red or blue by CK2 or GSK3β, respectively. In the absence of chemical shift changes on $T366^{P}$ upon phosphorylation of S361−T363 and reciprocally on $S361^{U}$−$T363^{U}$ upon phosphorylation of T366, $T366^{P}$ in species B′−E′ (blue box) are overlapped in the spectra as well as species A′ and B′ of each S361, S362 and T363 (dark-blue boxes). (B) Overlay of $^{1}H-^{15}N$ HSQC spectra recorded on the CK2-phosphorylated PTEN-Ctail sample in the time course of the GSK3β reaction from 0 to 9 h. Resonance assignment of the various phosphorylated species is indicated. (Inset) Time courses of the normalized amplitudes of $T366^{U}$ (species A′) and $T366^{P}$ (species B ′+ C′ + D′ + E′ = 1 − A′) resonances were fitted to single exponential functions (solid lines). (C) Overlay of HSQC spectra as in (B) but recorded for longer reaction times, 22 and 120 h. From 120 h onward, resonance shifts were observed, due to slight pH changes likely induced by ATP hydrolysis. (D) Amplitudes (not normalized) of the average resonance signals for each species A′+B′, C′, D′ and E′ are plotted as a function of the GSK3β reaction time. Error bars correspond to the rms of the noise in the corresponding spectrum. The curves (solid lines) are the result of individual nonlinear least-squares fitting of the amplitudes $A' + B'$, C' and D' to their corresponding eqs (1a) + (1b), (1c) and (1d) given in SI. The apparent rate constants are given in Table 1 (note the poor accuracy on $k'_{app,4}$ determination).

CK2-phosphorylated PTEN-Ctail. In the series of HSQC spectra recorded while the GSK3β reaction proceeds, $T366^{U}$ resonance disappears *via* a single exponential decay, while $T366^{P}$ resonance concomitantly appears *via* a single exponential growth with the same apparent rate constant (Figure 3B and Inset). The neighboring resonances (D368 and V369) disappear and reappear nearby with the same kinetics as $T366^{U}$ and $T366^{P}$. No time lag is observed in the appearance of the phosphorylated species $T366^{P}$, a feature attributed to the full phosphorylation of a priming residue, S370, in this sample. Extracting the apparent rate constant $k_{app}{}^{T366}$ by fitting the normalized amplitudes of the representative species $T366^{U}$ and $T366^{P}$ to single exponential functions (as described above for S370) gives an average and standard deviation of 0.43 ± 0.03

dx.doi.org/10.1021/ja310214g | J. Am. Chem. Soc. 2012, 134, 20533−20543

h^{-1} in our conditions (see Table 1). Note that the apparent rate constants for the GSK3β reaction are not directly comparable to the ones obtained for the CK2 reaction, due to the arbitrary concentration of kinases used in the *in vitro* experiment (8 and 39 nM for CK2 and GSK3β, respectively).

Surprisingly, the second GSK3β phosphorylated resonance peak S362^{P} (mentioned above) starts disappearing after about 20 h with the concomitant appearance of a new set of signals. From time 0 to longer reaction times (Figure 3C), we observed the ordered apparition of species A′−E′ corresponding to unphosphorylated (A′), mono-T366^{P} (B′), bi-T366^{P}-S362^{P} (C′), tri-T366^{P}-S362^{P}-S361^{P} (D′) and tetra-phosphorylated species T366^{P}-S362^{P}-S361^{P}-T363^{P} (E′), as defined in Figure 3A. Kinetics are consistent with the following sequential enzymatic reaction model:

$$A' \xrightarrow{k'^{\,T366}_{app,1\,GSK3\beta}} B' \xrightarrow{k'^{\,S362}_{app,2\,GSK3\beta}} C' \xrightarrow{k'^{\,S361}_{app,3\,CK2}} D' \xrightarrow{k'^{\,T363}_{app,4\,CK2}} E' \qquad (2)$$

We came to this conclusion for the following reasons: (i) phosphorylation of S361, S362 and T363 does not induce chemical shift changes on T366^{P}, so that a single resonance peak is observed for T366^{P}, whatever the phosphorylation states of S361 to T363 residues. So, its kinetics is described (see above) by a single exponential function defined by eq (1a) of the SI, corresponding to the sum of species B′ + C′ + D′ + E′ = 1 − A′. (ii) Similarly, phosphorylation of T366 does not induce chemical shift changes on S361, S362 and T363, so that species A′ and B′ overlap for the latter residues. Therefore, as shown in Figure 3A, we can "visualize" in the overlay of HSQC spectra (Figure 3C) species A′ + B′ *via* three resonance signals corresponding to unphosphorylated residues S361^{U}, S362^{U} and T363^{U}, species C′ *via* two unphosphorylated residues S361^{U} and T363^{U} and one phosphorylated residue S362^{P}, species D′ *via* one unphosphorylated residue T363^{U} and two phosphorylated residues S361^{P} and S362^{P} and species E′ *via* three unassigned small resonance signals that likely correspond to phosphorylated residues S361^{P}, S362^{P} and T363^{P}. The cascade of events is also clearly visible on the neighboring S360 resonance, which is slightly shifted upon each phosphorylation step, except upon the first one at T366. Interestingly, prior preliminary mass spectrometry experiments revealed the incorporation of a total of nine phosphoryl groups in PTEN-Ctail (Figure S4 in SI), in agreement with the NMR observation of the late phosphorylation events at S361 and T363 in addition to the seven *bona fide* phosphorylation sites. By incubating a CK2-phosphorylated sample at 60 °C for 20 min to inactivate CK2 prior addition of GSK3β, no phosphorylation of S361 and T363 was detected. However, adding a new aliquot of CK2 kinase in this sample induced successive phosphorylation of these two sites, which demonstrates that S361 and T363 are CK2-dependent phosphorylation sites (see Figure S5 in SI). Similarly, prior modification at S361 and/or T363 could in turn induce modification at S360. However, resonance signals of such a penta-phosphorylated species were not observed. Although the reaction is not complete, the apparent rate constants $k'_{app,2}$ to $k'_{app,4}$ are extracted from individual nonlinear least-squares fitting of non-normalized amplitudes A' + B', C', and D' to their corresponding equation ((1a) + (1b), (1c) and (1d) of SI) by fitting an additional parameter A_0' for each species (see Figure 3D and Materials and Methods). This leads to $k'^{\,S362}_{app,2\,GSK3\beta}$ = 0.193 ± 0.010 h^{-1}, $k'^{\,S361}_{app,3}$ = 0.012 ± 0.001 h^{-1} and an upper limit of $k'^{\,T363}_{app,4}$ < 0.006 h^{-1} in our conditions and with different relative time scales for GSK3β and CK2 reactions (Table 1). Very similar kinetics for all phosphorylation steps and the formation of the same intermediate phosphorylated states are obtained upon sequential or simultaneous addition of CK2 and GSK3β. However, the NMR analysis is simplified in the former case.

In conclusion, our *in vitro* data show that prior phosphorylation by CK2 at S370 allows phosphorylation by GSK3β at T366 and in turn at S362, which promotes, later in time, further ordered modifications at S361^{P} and T363^{P} by CK2 *via* a distributive kinetic mechanism →S370^{P}→T366^{P}→S362^{P}→S361^{P}→T363^{P} (Figure 5).

Observation of the Dynamic Process of PTEN-Ctail Multisite Phosphorylation in Neuroblastoma Cell Extracts. Finally, we intended to assess if the multisite phosphorylation events also take place in cellular extracts of human neuroblastoma, if they follow a similar ordered process and if this pattern could be accounted for by the likely and sole presence of CK2 and GSK3β kinases in these extracts. Human neuroblastoma cells were chosen because they express the kinases CK2 and GSK3β (Figure S7 in SI) and they constitute a suitable model for studying the role of PTEN in neuritogenesis.[27,28] Human neuroblastoma SH-SY5Y cell extracts[29] were prepared as described in Materials and Methods. From 10^8 differentiated cells, a total protein concentration of 12 to 15 mg/mL was quantified in the extracts. The NMR sample was prepared by adding U−^{15}N/^{13}C-labeled PTEN-Ctail (50 μM, final concentration) to the neuroblastoma cell extracts (see Materials and Methods). ^{1}H−^{15}N HSQC spectra were rapidly recorded after PTEN-Ctail was added to the extracts. The spectra display rather narrow ^{1}H and ^{15}N line-widths despite the higher viscosity of this cellular medium. After 30 h, no more changes were observed in the spectra.

Compared to the spectrum of unphosphorylated PTEN-Ctail *in vitro*, we observed the appearance of many new resonance peaks (Figure 4A). Most of them formed a "pattern" globally similar to the one observed in the overlay of HSQC recorded *in vitro* during the CK2 and GSK3β reactions (Figure S2 in SI and Figure 3C). By analogy, we assigned resonances of species A−E (as defined in Figure 2A), corresponding to phosphorylation within the S380−S385 cluster. We also assigned resonances of species A′−D′ (as defined in Figure 3A), corresponding to phosphorylation of T366, S362 and S361. Species E′ was barely detected by a fourth S360 resonance (star below threshold in Figure 4A), suggesting that T363 is likely phosphorylated at a low level. Under various conditions (large excess of ATP, phosphatase inhibitors, changes in the solvent or in the reaction temperature), higher phosphorylation levels could not be reached. The overall similarity with the pattern of resonances observed *in vitro* indicates that, in these cellular extracts, the phosphorylation process is essentially sequential, involving the same intermediate phosphorylation species, →S385^{P}→S380^{P}→T383^{P}→T382^{P} and →S370^{P}→T366→S362→S361^{P}→T363^{P}. It is most probably controlled by endogenous CK2 and GSK3β kinases present in the extracts (Figure 5).

However, some differences are observed with the *in vitro* experiments, such as the detection of five new Ser/Thr resonance peaks (Figure 4A). Four of them (labeled with magenta G in Figure 4A) are in the vicinity of S380^{U}, T382^{U}, T383^{P} and S385^{P} resonances. They most likely correspond to the doubly phosphorylated species S380^{U}−T382^{U}−T383^{P}−S385^{P} (called species G). As a qualitative argument for its identification, the changes in chemical shifts of each of S380^{U},

dx.doi.org/10.1021/ja310214g | J. Am. Chem. Soc. 2012, 134, 20533−20543

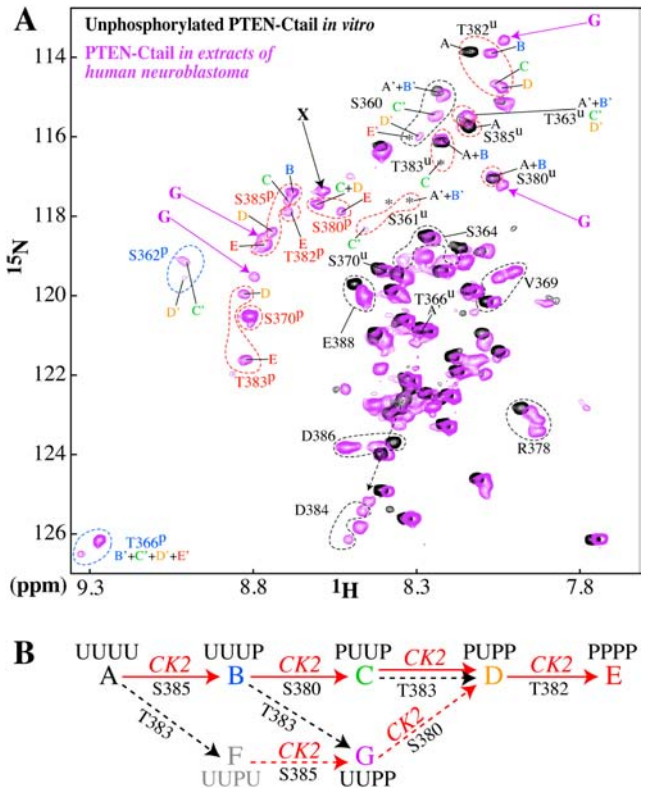

Figure 4. Detection of PTEN-Ctail phosphorylation in neuroblastoma cell extracts. (A) Superposition of $^{1}H-^{15}N$ HSQC spectra of PTEN-Ctail recorded in neuroblastoma cell extracts after 30 h of phosphorylation by endogenous kinases (magenta, pH 7.5) and *in vitro* on its unphosphorylated state (black, pH 6.7). Slight differences in amide chemical shifts compared to the *in vitro* spectra are likely due to the pH difference. Resonances appearing below the threshold level of the plot are indicated by a star (*). Assignment of the intermediate phosphorylated states corresponding to species A, B, C, D, E for the S380−S385 cluster and to species A′, B′, C′, D′, E′ for the S361−T366 cluster is indicated with the color-coding of Figures 2 and 3. Set of resonances corresponding to phosphorylated residues by CK2 and GSK3β in cell extracts are surrounded in red and blue, respectively. The five new Ser/Thr resonance peaks are indicated by a magenta G or a black X (see text). (B) Proposed branched model in the S380−S385 cluster to account for the new species G. Black dotted arrows denote the alternative pathway possibly controlled by a kinase other than CK2 or GSK3β. The putative species F in gray is not detected. In each species, U or P indicates the phosphorylation state of S380, T382, T383 and S385.

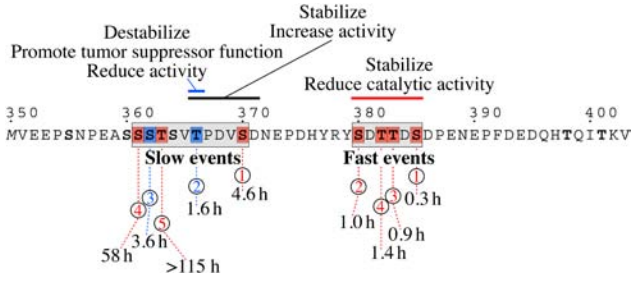

Figure 5. Two independent cascades of ordered phosphorylation events at the PTEN-Ctail. All Ser and Thr residues are shown in bold. The phosphorylated Ser/Thr (detected in this study *in vitro* or in cell extracts) are boxed and ordered according to their order of apparition within each cluster (CK2 in red and GSK3β in blue). The half-life time (log $2/k_{app}$) of each event inferred from the *in vitro* experiments is indicated. Gray boxes underline the two independent cascades. The functional role of a specific phosphorylation is indicated at the top (see text).

$T382^{U}$, $T383^{P}$ and $S385^{P}$ in the new species G with respect to their chemical shifts in species A to E agree well to what would be expected in relation to the distance to a phosphorylated residue. The new species G lays off-pathway from the linear chain reaction controlled *in vitro* by CK2 and GSK3β only. This suggests a more complex branched mechanism, following the model described in Figure 4B. The species G could arise either from species B or from species A through the transient intermediate species $S380^{U}-T382^{U}-T383^{P}-S385^{U}$ (called species F). The latter is not detected in our experiment, possibly because of its too short lifetime, due to the fast $S385^{U}/S385^{P}$ conversion by CK2 (in the same manner as species A has disappeared at this time of the reaction). As compared to the linear model, this branched mechanism would imply a change in the relative time course of species A to E and, intuitively, a shunt in the accumulation of species C. This is indeed the case: as seen in Figure 4A, the amplitudes of the resonance peaks of species C are significantly smaller than that measured for species B and D, a situation never observed along the time course of the *in vitro* reaction (see Figure 2C). Therefore, in the cell extracts, the kinetics in the S380−S385 cluster must change beyond a simple scaling factor of the apparent rate constants determined *in vitro*. Note that, by simulating the enzymatic chain reaction (see SI and Figure S8), we show that, under the conditions prevailing in our *in vitro* experiments, changing the initial substrate or kinase concentration should change only the global rate of the reaction but should not affect the apparent rate constants relative to each other. The absence of this alternative pathway *in vitro* further suggests the contribution of a kinase other than CK2 or GSK3β present in the cell extracts, acting on T383. Note that this species G could arise from dephosphorylation at S380 in species D, but this hypothesis is improbable due to the use of a phosphatase inhibitor cocktail. Finally, a fifth new peak appears also in the region of the phosphorylated Ser/Thr (black X in Figure 4A). This single peak indicates that an isolated site of PTEN-Ctail is likely phosphorylated by a kinase specifically different from CK2 and GSK3β as well. Further experiments are in progress to test these hypotheses.

In conclusion, our data indicate (i) that endogenous kinases present in the neuroblastoma cell extracts are able to phosphorylate PTEN-Ctail, (ii) that the phosphorylation cascade controlled by CK2 and GSK3β proceeds according to the distributive ordered process established *in vitro*, (iii) that a branched pathway occurs involving the phosphorylation of T383, possibly by another kinase, and consequently, (iv) that the relative apparent rate constants within the S380−S385 cluster must change beyond a simple scaling factor of the $k_{app,1}$ to $k_{app,4}$ values established *in vitro*. Thus, the data obtained in cell extracts are essentially compatible with the *in vitro* data but also highlight the consequences of a more physiological context in the extracts.

DISCUSSION

Summary. Using NMR spectroscopy, we have deciphered the multisite phosphorylation pattern of PTEN-Ctail by CK2 and GSK3β. We unambiguously identified, both *in vitro* and in human neuroblastoma cell extracts, nine phosphorylation sites, in agreement with the incorporation of nine phosphoryl groups

dx.doi.org/10.1021/ja310214g | J. Am. Chem. Soc. 2012, 134, 20533−20543

that we preliminary detected by mass spectrometry. Following by NMR the formation of intermediate phosphorylated species *in vitro*, we derived apparent rate constants (specific for our conditions) for each phosphorylation step and showed that two cascades of events occur independently. The first one is controlled by CK2 and corresponds to the path S385→S380→T383→T382. The second is slower and occurs in the order S370→*T366*→*S362*→S361→T363 through the action of CK2, GSK3β (italic) and CK2 again (Figure 5). The latter appears as slower since the apparent rate constant of its first event on S370 is more than 10-fold smaller than that of S385 by the same kinase. In the cellular extracts, the two cascades follow the same ordered and distributive process as observed *in vitro* and are most likely controlled by endogenous CK2 and GSK3β, the dominant kinases phosphorylating PTEN. However, the detection of a new off-pathway phosphorylated species suggests the phosphorylation of T383 *via* an alternative pathway in the cellular extracts, possibly controlled by another kinase.

Comparison with Literature. Seven of these sites (S370, S380, T382, T383 and S385 by CK2 and S362 and T366 by GSK3β) were previously reported using traditional techniques. However, they were only detected as various subsets and to various extents, even *in vitro*. For instance, S370 and S385 were identified as major phospho sites *in vitro* and *in vivo*.[6,9,12] Astonishingly, phosphoamino acid analysis, mass spectrometry and autoradiography experiments did not permit to detect phosphorylation at S380 *in vitro*.[12] Similarly, phospho-specific antibodies against S362 failed to detect phosphorylation at S362 either in cells or *in vitro*.[16] These apparent contradictions with our NMR data are rather the consequences of technical limitations than of an actual absence of modification. This clearly emphasizes the advantage of NMR upon other techniques to unambiguously identify the whole pattern of modifications. To our knowledge, the two CK2-phospho-sites S361 and T363, which we observed both *in vitro* and in neuroblastoma cell extracts, had never been reported yet, probably because of an apparent low population due to their slow kinetics. Functional experiments (beyond the scope of this paper) are nevertheless required to assess the biological relevance of those late occurring phosphorylation events.

Consensus and Predictions. These nine phosphorylation sites lie within a CK2 or GSK3β consensus motif[17−19,30] and could have been somehow predicted. For S361 and T363 sites possibly controlled by CK2, the acidic charges (represented by phosphorylated Ser/Thr) are less abundant between positions $n - 1$ to $n + 4$, which could justify their slower kinetics. However, in all cases, precise information on the phosphorylation kinetics was missing and convincing biochemical pathways could not be established. Our results illustrate, for example, two counterintuitive experimental facts: First, S380, with an unphosphorylated T at the crucial $n + 3$ position, is processed *in vitro* with a 4-fold faster apparent rate constant than S370 that possesses a more favorable residue, E, at the same relative position; second, the order S385−S380−T383−T382 is determined experimentally whereas, from the CK2 consensus sequence, an order from the C- to the N-terminus would be intuitively expected in the S380−S385 cluster. Although the definition of consensus sequences from systematic studies can greatly facilitate the prediction of potential sites, unambiguous identification of phosphorylation sites as well as determination of phosphorylation order and efficiency cannot rely on such predictions without experimental evidence. PTEN-Ctail can be taken as an example where other determinants modulate phosphorylation order and efficiency. Furthermore, in this case, the presence of strictly ordered phosphorylation pathways has another consequence: Any point mutation of Ser/Thr residues differentially affects the cascade of phosphorylation events in the downstream pathway. For example, the mutation S380A does not block the cascade but significantly delays the formation of the fully phosphorylated species (see Figure S3 in Supporting Information). Consequently, the local modification might not be directly responsible for the observed functional outcome.

Multisite Phosphorylation and Distributive Mechanism. The observation by NMR of each intermediate phosphorylation species of PTEN-Ctail is clearly characteristic of a distributive mechanism. Although such a mechanism is less energetically favorable than a processive mechanism,[31] it can exert critical regulatory functions in cellular signaling. Distributive multisite phosphorylation process introduces a dependence on enzyme concentration such that a small change in kinase (or phosphatase) concentration leads to a large change in the proportion of phosphorylated substrate. It was proposed that this ultrasensitive behavior produces a switch-like response, the regulatory outcome being an all-or-none cell decision.[32,33] More recently, a new notion has been introduced.[34] Above a certain threshold in the kinase to phosphatase ratio, the amount of fully phosphorylated species increases so that the response may increase in a gradual manner, in contrast to the situation generated by a switch.[35] In this perspective, phosphorylation at S361 and T363 might have a biological relevance during certain cell regulation processes. It was also shown that an ordered phosphorylation affecting many sites in theory leads to steeper response curves than random phosphorylation.[36] This is indeed observed here for PTEN CK2-sites S380−S385 compared to S370.

Functional Role of Each Cluster. So far, phosphorylation within the S380−S385 cluster was shown to stabilize PTEN and to reduce its catalytic activity.[5,6] On the contrary, the function of phosphorylation of S370 and T366 is still unclear. T366 was found phosphorylated *in vivo* but to a lower extent than S370 and S385.[9] On one hand, phosphorylation of T366 by GSK3β was reported to lead to PTEN destabilization,[16] to promote its tumor suppressor function and to reduce its activity in 293T cells.[12] On the other hand, Xu et al. have shown more recently that another kinase, Plk3, phosphorylates both S370 and T366 *in vitro* and in murine embryonic fibroblasts and that Plk3-mediated phosphorylation is associated with PTEN stabilization and increase of PTEN activity.[13] Very recently, Tibarewal et al. showed that PTEN dephosphorylates its C-terminal tail at T366, and that this autophosphatase activity increases its lipid phosphatase activity sufficiently to inhibit cell invasion in glioblastoma cell lines.[37] Taken together, these functional studies highlight distinct functional roles for the phosphorylation events within the two clusters that might be cell-/stimulus-dependent (Figure 5). Our findings of two cascades occurring independently, on different time scales and triggered by modifications of S385 and S370 respectively suggest that these events may function as two delay timers activating different (or time-delayed) regulatory responses.

Additional Kinases. Due to their position upstream of the cascade, S370 and S385 appear as "major" phosphorylation sites, as suggested previously *in vitro* and *in vivo*.[6,9,38] It was even proposed that S370 and S385 are constitutively phosphorylated and may serve as priming additional phosphorylation events, whereas S380, T382 and T383 may be

regulated by a balance between kinases and phosphatases, thereby controlling PTEN stability and activity.[5,7,38] CK2 and GSK3β were initially reported as the dominant kinases phosphorylating PTEN, but other kinases are also implicated, such as MAST family,[14] LKB1,[15] CK1[12] and Plk3.[13] Our observation of new phosphorylated species in the cellular extracts as compared to *in vitro* suggests indeed the contribution of at least one additional kinase acting in particular on T383. The functional importance of this residue has been highlighted in several studies. The phosphorylation state of T383 was shown to control the activity of PTEN in a manner independent of its lipid phosphatase activity:[39] PTEN was suggested to dephosphorylate itself on T383[39] and LKB1 to be a kinase able to phosphorylate T383 *in vitro*.[15]

Advantages of High-Resolution NMR Spectroscopy. An increasing number of essential proteins appears to display disordered regulatory sequences encompassing stretches of potentially phosphorylated residues, such as PTEN. NMR appears then as a technique of choice to study such complex multisite phosphorylation patterns. Although tyrosine phosphorylation, unlike serine or threonine phosphorylation, does not induce a large downfield shift of the amide proton chemical shift,[40] phosphorylation of this residue can be detected by ^{1}H, ^{15}N chemical shift changes on the neighboring residues or alternatively in ^{1}H−^{13}C HSQC spectra by the expected large downfield shifts of the tyrosine Hε and Cε chemical shifts.[40,41] Besides its advantages for the unambiguous detection of phosphorylated Ser/Thr/Tyr residues, we show here that NMR further allows deciphering in a time-dependent manner the mechanism of multisite protein phosphorylation, even for adjacent or closely spaced substrate residues. The property and sensitivity of the NMR resonance signal allows (i) detecting the kinase-released intermediate species in a distributive mechanism, (ii) following their transient formation in the time course of the reaction and (iii) extracting an apparent rate constant for each step. In the light of the numerous analytical studies on phosphorylation mechanisms,[35,42,43] such an experimental approach appears promising to explore the highly dynamical nature of phosphorylation processes in more physiological conditions. In spite of being a biased *ex cellulo* system, NMR experiments performed in cell extracts (combined with *in vitro* experiments) constitute a first step toward investigating the cooperative role of kinases and phosphatases in intact cellular systems by in-cell NMR using cell-penetrating substrate derivative constructs. Finally, these results bring an unprecedented temporal dimension on the analysis of PTEN phosphorylation cascade. It will certainly shed new light on its role in finely timing cellular events.

MATERIALS AND METHODS

PTEN-Ctail Expression and Purification. Recombinant U−^{15}N/^{13}C-labeled PTEN-Ctail (encompassing residues V351−V403 of human PTEN) was produced in *E. coli* as described in the Supporting Information.

Mass Spectrometry. SELDI-TOF-MS was performed as described in the Supporting Information.

***In Vitro* CK2- and GSK3β-Phosphorylation Assays by NMR.** A NMR sample containing 250 μL of U−^{15}N/^{13}C-labeled PTEN-Ctail was prepared at 120 μM, and the pH was adjusted to 6.7. All the NMR experiments were carried out at 25 °C on a Varian Inova 600-MHz spectrometer equipped with a cryoprobe. Standard 3D triple resonance NMR experiments were recorded for backbone resonance assignment of the unphosphorylated form. Phosphorylation of PTEN-Ctail by CK2 kinase was monitored by adding to the PTEN-Ctail sample 1 μL of 0.1 mg/mL (8 nM) unlabeled CK2 kinase, 2 mM ATP and 10 mM $MgCl_2$-containing kinase buffer. A series of ^{1}H−^{15}N HSQC was regularly recorded until the CK2 reaction stopped (after 21 h) and a set of 3D experiments was recorded for resonance assignment of the CK2-phosphorylated PTEN-Ctail. Phosphorylation by GSK3β was assayed by adding to the previous sample 5 μL of 0.1 mg/mL (39 nM) unlabeled GSK3β kinase. This amount of kinase was adjusted so that the CK2 and the GSK3β reactions occur on a similar time scale. A series of ^{1}H−^{15}N HSQC was again regularly recorded while the GSK3β reaction proceeded. After 9 h, a set of 3D experiments was recorded for resonance assignment of the CK2- and GSK3β-phosphorylated PTEN-Ctail. In between each 3D experiments, ^{1}H−^{15}N HSQC were continuously recorded until 140 h. Finally, reaction by CK2 and GSK3β was similarly monitored on a comparable sample but after simultaneous addition of 8 nM of CK2 and 39 nM of GSK3β. Data processing and analysis were carried out using NMRPipe[44] and NMRView.[45]

Fitting Procedure. From the series of HSQC, the resonance amplitudes (volumes) were measured for each residue in each phosphorylated species as a function of time. For each residue, amplitude normalization was achieved using a residue-specific normalization constant A_0, so that the sum of the amplitudes of the different phosphorylated states of this residue equals 1 (for instance, for residue n of the S380−S385 cluster, so that $(A_n + B_n + C_n + D_n + E_n) = A_{0,n} = 1$). First, for each peak representative of species A, an apparent rate constant $k_{app,1}$ was extracted by nonlinear least-squares fitting of its amplitudes A (weighted by the rms of the noise in the corresponding spectrum) to eq (1a) of Supporting Information, using a simplex or Levenberg−Marquardt algorithm. Value of $k_{app,1}$ was derived from the average and standard deviation from these individual fits. Second, fixing $k_{app,1}$ to this value, $k_{app,2}$ was similarly extracted from the average and standard deviation over individual fits of each series of amplitudes B to eq (1b). A two-floating parameter fit of both $k_{app,1}$ and $k_{app,2}$ led to very similar results. Third, fixing $k_{app,1}$ and $k_{app,2}$ to the preceding values, $k_{app,3}$ was extracted from the average and standard deviation over individual fits of each series of amplitudes C to eq (1c), also leading to similar values as extracted from a three-floating parameter fit of $k_{app,1}$, $k_{app,2}$ and $k_{app,3}$. Fourth, fixing $k_{app,1}$, $k_{app,2}$ and $k_{app,3}$ to the preceding values, $k_{app,4}$ was extracted from the average and standard deviation over individual fits of each series of amplitudes D to eq (1d) and, fifth, of each series of amplitudes E to eq (1e). In the HSQC spectra, when resonances belonging to a same residue were entirely or partially overlapped in several species (e.g., T383$^{U}(A + B)$ or R378$(C + D + E)$), the global volume was considered and the fit was performed to the corresponding sum of equations ((1a) + (1b) or (1c) + (1d) + (1e), respectively). Being aware that some combinations such as (1c) + (1d) + (1e) = 1 − (1a) − (1b) are dependent on $k_{app,1}$ and $k_{app,2}$ only, fitting such overlapped resonances led to very similar apparent rate constants for these two parameters. Such considerations can be helpful for proteins concerned by severe spectral overlapping. Finally, $k_{app,1}$, $k_{app,2}$, $k_{app,3}$ and $k_{app,4}$ were extracted from a global fit of the average amplitudes A−E to eqs (1a)−(1e), and standard errors were estimated from Monte Carlo simulations, leading to very similar values as the independent fit of each species. All the values of the apparent rate constants are given in Table S1(SI) for the cluster S380−S385. For the cluster S361−T366, a similar procedure was performed, except that $k'_{app,1}$ (for T366) was first extracted from a fit to single exponential functions (see text). Then, for $k'_{app,2}$, $k'_{app,3}$ and $k'_{app,4}$, although the reaction is not complete, the average amplitudes $A' + B'$, C' and D' were fitted independently to their corresponding eqs (1a) + (1b), (1c), and (1d), respectively, with a floating normalization parameter A_0 for each species (see Table S3 in SI).

Phosphorylation Assays in Neuroblastoma Cell Extracts by NMR. Extracts of human neuroblastoma SH-SY5Y cells[29] were prepared as described in the SI. From 10^8 differentiated cells, a total protein concentration of 12−15 mg/mL was quantified in the cell extracts. A NMR sample of PTEN-Ctail in neuroblastoma cell extracts was prepared by adding 25 μL of U−^{15}N/^{13}C-labeled PTEN-Ctail stock solution, 10% D_2O, 100 mM Tris-HCl pH 7.5, 10 mM $MgCl_2$-containing kinase buffer and 15 mM ATP to 170 μL of cell extracts.

dx.doi.org/10.1021/ja310214g | J. Am. Chem. Soc. 2012, 134, 20533−20543

The total volume was 300 μL, leading to a final PTEN-Ctail concentration of 50 μM. The pH was kept at 7.5, close to physiological conditions. The extract sample was rapidly transferred into a Shigemi NMR microtube for NMR measurements at 25 °C. A series of $^{1}H-^{15}N$ HSQC (3−6 h acquisition time) was regularly recorded until modifications no longer could be observed in the spectra (30 h).

■ ASSOCIATED CONTENT

Ⓢ Supporting Information

Details on PTEN-Ctail expression and purification, SELDI-TOF-MS experiments, *in vitro* phosphorylation assay by NMR, preparation of neuroblastoma cell extracts and on numerical simulations of the sequential enzymatic chain reaction; Equations of the linear five-state model; Figures of chemical shift differences between unphosphorylated and phosphorylated PTEN-Ctail, full HSQC spectra recorded in the time course of the CK2 reaction, kinetics for the S380A mutant, mass spectrometry profiles, identification of S361 and T363 as CK2-phosphorylation sites, kinetics for the S380A/T382A/T383A/S385A mutant, Immunoblots and numerical simulations; detailed tables of the apparent rate constants. This material is available free of charge via the Internet at http://pubs.acs.org.

■ AUTHOR INFORMATION

Corresponding Author

florence.cordier@pasteur.fr

Present Address

□Present address: Department of NMR assisted (FMP Berlin), 13125 Berlin, Germany.

Notes

The authors declare no competing financial interest.

■ ACKNOWLEDGMENTS

This work was supported by the CNRS and grants from the Institut Pasteur, Agence Nationale pour la Recherche (PATHO-PDZ), and Institut Carnot Pasteur Maladies Infectieuses (NeuroVita). E.T. is a recipient of fellowships from the Ministère de l'Enseignement Supérieur et de la Recherche and from the Fondation pour la Recherche Médicale. We thank N. Kellershohn for valuable discussions, J. D'Alayer for help with mass spectrometry experiments and S. Baeriswyl for careful proofreading of the manuscript.

■ ABBREVIATIONS

PTEN, phosphatase and tensin homologue deleted on chromosome 10; CK2, casein kinase 2; GSK3β, glycogen synthase kinase-3 β; HSQC, heteronuclear single quantum correlation

■ REFERENCES

(1) Salmena, L.; Carracedo, A.; Pandolfi, P. P. *Cell* **2008**, *133*, 403−414.
(2) Park, K. K.; Liu, K.; Hu, Y.; Smith, P. D.; Wang, C.; Cai, B.; Xu, B.; Connolly, L.; Kramvis, I.; Sahin, M.; He, Z. *Science* **2008**, *322*, 963−966.
(3) Gericke, A.; Munson, M.; Ross, A. H. *Gene* **2006**, *374*, 1−9.
(4) Leslie, N. R.; Batty, I. H.; Maccario, H.; Davidson, L.; Downes, C. P. *Oncogene* **2008**, *27*, 5464−5476.
(5) Vazquez, F.; Ramaswamy, S.; Nakamura, N.; Sellers, W. R. *Mol. Cell. Biol.* **2000**, *20*, 5010−5018.
(6) Torres, J.; Pulido, R. *J. Biol. Chem.* **2001**, *276*, 993−998.
(7) Tolkacheva, T.; Boddapati, M.; Sanfiz, A.; Tsuchida, K.; Kimmelman, A. C.; Chan, A. M. *Cancer Res.* **2001**, *61*, 4985−4989.
(8) Vazquez, F.; Grossman, S. R.; Takahashi, Y.; Rokas, M. V.; Nakamura, N.; Sellers, W. R. *J. Biol. Chem.* **2001**, *276*, 48627−48630.
(9) Miller, S. J.; Lou, D. Y.; Seldin, D. C.; Lane, W. S.; Neel, B. G. *FEBS Lett.* **2002**, *528*, 145−153.
(10) Das, S.; Dixon, J. E.; Cho, W. *Proc. Natl. Acad. Sci. U.S.A.* **2003**, *100*, 7491−7496.
(11) Vazquez, F.; Matsuoka, S.; Sellers, W. R.; Yanagida, T.; Ueda, M.; Devreotes, P. N. *Proc. Natl. Acad. Sci. U.S.A.* **2006**, *103*, 3633−3638.
(12) Al-Khouri, A. M.; Ma, Y.; Togo, S. H.; Williams, S.; Mustelin, T. *J. Biol. Chem.* **2005**, *280*, 35195−35202.
(13) Xu, D.; Yao, Y.; Jiang, X.; Lu, L.; Dai, W. *J. Biol. Chem.* **2010**, *285*, 39935−39942.
(14) Valiente, M.; Andres-Pons, A.; Gomar, B.; Torres, J.; Gil, A.; Tapparel, C.; Antonarakis, S. E.; Pulido, R. *J. Biol. Chem.* **2005**, *280*, 28936−28943.
(15) Mehenni, H.; Lin-Marq, N.; Buchet-Poyau, K.; Reymond, A.; Collart, M. A.; Picard, D.; Antonarakis, S. E. *Hum. Mol. Genet.* **2005**, *14*, 2209−2219.
(16) Maccario, H.; Perera, N. M.; Davidson, L.; Downes, C. P.; Leslie, N. R. *Biochem. J.* **2007**, *405*, 439−444.
(17) Pinna, L. A. *J. Cell Sci.* **2002**, *115*, 3873−3878.
(18) Frame, S.; Cohen, P. *Biochem. J.* **2001**, *359*, 1−16.
(19) Frame, S.; Cohen, P.; Biondi, R. M. *Mol. Cell* **2001**, *7*, 1321−1327.
(20) Kirkpatrick, D. S.; Gerber, S. A.; Gygi, S. P. *Methods* **2005**, *35*, 265−273.
(21) Singh, S.; Springer, M.; Steen, J.; Kirschner, M. W.; Steen, H. *J. Proteome Res* **2009**, *8*, 2201−2210.
(22) Boehm, M. E.; Seidler, J.; Hahn, B.; Lehmann, W. D. *Proteomics* **2012**, *12*, 2167−2178.
(23) Selenko, P.; Frueh, D. P.; Elsaesser, S. J.; Haas, W.; Gygi, S. P.; Wagner, G. *Nat. Struct. Mol. Biol.* **2008**, *15*, 321−329.
(24) Landrieu, I.; Lacosse, L.; Leroy, A.; Wieruszeski, J. M.; Trivelli, X.; Sillen, A.; Sibille, N.; Schwalbe, H.; Saxena, K.; Langer, T.; Lippens, G. *J. Am. Chem. Soc.* **2006**, *128*, 3575−3583.
(25) Leroy, A.; Landrieu, I.; Huvent, I.; Legrand, D.; Codeville, B.; Wieruszeski, J. M.; Lippens, G. *J. Biol. Chem.* **2010**, *285*, 33435−33444.
(26) Liokatis, S.; Dose, A.; Schwarzer, D.; Selenko, P. *J. Am. Chem. Soc.* **2010**, *132*, 14704−14705.
(27) Prehaud, C.; Wolff, N.; Terrien, E.; Lafage, M.; Megret, F.; Babault, N.; Cordier, F.; Tan, G. S.; Maitrepierre, E.; Menager, P.; Chopy, D.; Hoos, S.; England, P.; Delepierre, M.; Schnell, M. J.; Buc, H.; Lafon, M. *Sci. Signaling* **2010**, *3*, ra5.
(28) Terrien, E.; Chaffotte, A.; Lafage, M.; Khan, Z.; Prehaud, C.; Cordier, F.; Simenel, C.; Delepierre, M.; Buc, H.; Lafon, M.; Wolff, N. *Sci. Signaling* **2012**, *5*, ra58.
(29) Loh, S. H. Y.; Francescut, L.; Lingor, P.; Bahr, M.; Nicotera, P. *Cell Death Differ.* **2008**, *15*, 283−298.
(30) Sarno, S.; Vaglio, P.; Cesaro, L.; Marin, O.; Pinna, L. A. *Mol. Cell. Biochem.* **1999**, *191*, 13−19.
(31) Patwardhan, P.; Miller, W. T. *Cell. Signalling* **2007**, *19*, 2218−2226.
(32) Ferrell, J. E., Jr. *Trends Biochem. Sci.* **1996**, *21*, 460−466.
(33) Ferrell, J. E., Jr.; Machleder, E. M. *Science* **1998**, *280*, 895−898.
(34) Nash, P.; Tang, X.; Orlicky, S.; Chen, Q.; Gertler, F. B.; Mendenhall, M. D.; Sicheri, F.; Pawson, T.; Tyers, M. *Nature* **2001**, *414*, 514−521.
(35) Gunawardena, J. *Proc. Natl. Acad. Sci. U.S.A.* **2005**, *102*, 14617−14622.
(36) Salazar, C.; Hofer, T. *FEBS J.* **2007**, *274*, 1046−1061.
(37) Tibarewal, P.; Zilidis, G.; Spinelli, L.; Schurch, N.; Maccario, H.; Gray, A.; Perera, N. M.; Davidson, L.; Barton, G. J.; Leslie, N. R. *Sci. Signaling* **2012**, *5*, ra18.
(38) Odriozola, L.; Singh, G.; Hoang, T.; Chan, A. M. *J. Biol. Chem.* **2007**, *282*, 23306−22315.
(39) Raftopoulou, M.; Etienne-Manneville, S.; Self, A.; Nicholls, S.; Hall, A. *Science* **2004**, *303*, 1179−1181.

(40) Bienkiewicz, E. A.; Lumb, K. J. *J. Biomol. NMR* **1999**, *15*, 203−206.
(41) Deshmukh, L.; Meller, N.; Alder, N.; Byzova, T.; Vinogradova, O. *J. Biol. Chem.* **2011**, *286*, 40943−40953.
(42) Salazar, C.; Hofer, T. *FEBS J.* **2009**, *276*, 3177−3198.
(43) Salazar, C.; Brummer, A.; Alberghina, L.; Hofer, T. *Trends Cell. Biol.* **2010**, *20*, 634−641.
(44) Delaglio, F.; Grzesiek, S.; Vuister, G. W.; Zhu, G.; Pfeifer, J.; Bax, A. *J. Biomol. NMR* **1995**, *6*, 277−293.
(45) Johnson, B. A.; Blevins, R. A. *J. Biomol. NMR* **1994**, *4*, 603−614.